Pharmacogn. Mag.
A multifaceted peer reviewed journal in the field of Pharmacognosy and Natural Products
www.phcog.com | www.phcog.net

ORIGINAL ARTICLE

Amygdalin Attenuates Neuroinflammatory Injury via Down-Regulating Toll-Like Receptors-2/Toll-Like Receptors-4-Nuclear Factor Kappa-B Signaling Pathway in BV2

Tong Sun[1], Jing-Jing Lu[2], Bi-Xu Wang[1], Xiao-Qing Ye[1], Lan Li[1], Fang-Mei Zhou[1], Hai-Tong Wan[3], Zhi-Shan Ding[1]

[1]School of Medical Technology and Information Engineering, Zhejiang Chinese Medical University, [2]College of Life Science, Zhejiang Chinese Medical University, Hangzhou 310053, Zhejiang, [3]Zhejiang Chinese Medical University Hangzhou 310053, China

Submitted: 23-Jan-2022 Revised: 23-Mar-2022 Accepted: 03-Aug-2022 Published: 23-Nov-2022

ABSTRACT

Background: Amygdalin is the essential component of the traditional Chinese medicinal drug peach kernel. The early studies of amygdalin are mainly focused on antitussive and tumor anti-tumor, but there are few studies on the treatment of neuroinflammation. **Objectives:** The purpose of this study was to explore the anti-inflammatory effect of amygdalin on lipopolysaccharide (LPS)-induced neuron–microglia and its protective mechanism for toll-like receptors (TLRs) signaling pathways. **Materials and Methods:** Griess, quantitative PCR, and flow cytometry were used to detect the influence of amygdalin on the release of inflammatory factors from BV2 mouse microglia (BV2 cells). The anti-inflammatory pathway of amygdalin was further explored by western blotting. At the same time, the effect of amygdalin on LPS-induced oxidative stress damage in BV2 cells was detected by WST-8 and fluorescence probe. **Results:** After LPS induction, the pro-inflammatory factors such as nitric oxide, interleukin-6, tumor necrosis factor-alpha, interleukin-1β, and recombinant NLR Family, Pyrin Domain Containing Protein3 were significantly increased. However, the levels were reversed significantly after treatment with amygdalin. In addition, amygdalin significantly inhibited the increase of TLR4, TLR2, and its downstream signal myeloid differentiation primary response gene 88 and P-NF-κB p65 in BV2 cells induced by LPS. Amygdalin can also reverse the abnormal expression of LPS-induced oxidative stress indexes such as cyclooxygenase-2, reactive oxygen species, and superoxide dismutase. **Conclusion:** Amygdalin may reduce the LPS-induced accumulation of pro-inflammatory substances via the down-regulating of the TLR2/TLR4-nuclear factor kappa-B signaling pathway.

Key words: Amygdalin, BV2 microglia, neuroinflammation, oxidative stress, TLRs signaling pathways

SUMMARY

- Neuroinflammation is the common pathogenic mechanism of many neurodegenerative diseases. With the characteristics of small side effects, multi-targets, and multi-links, traditional Chinese medicine has great potential in the treatment of neurodegenerative diseases.
- Amygdalin has anti-tumor, anti-fibrosis, anti-atherosclerotic, and other pharmacological effects. However, there are few studies on amygdalin in the treatment of neuroinflammation.
- Amygdalin may reduce the inflammation and oxidative damage of BV2 cells induced by LPS through TLR2/4-NF-κB pathway to play an immunomodulatory role.

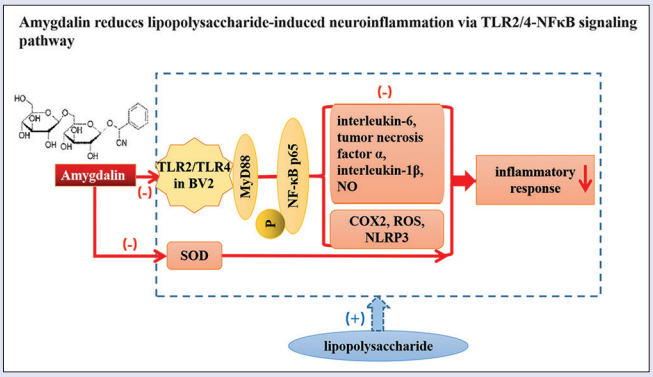

Abbreviations used: BV2 cells: BV2 mouse microglia; CNS: central nervous system; IL-6: interleukin-6; IL-1β: interleukin-1β; TNF-α: tumor necrosis factor-α; TLRs: Toll-like receptors; MyD88: Myeloid differentiation primary response gene 88; NF-κB: Nuclear factor kappa-B; NLRP3: Recombinant NLR Family, Pyrin Domain Containing Protein3; ROS: Reactive oxygen species; SOD: Superoxide dismutase; COX-2: Cyclooxygenase; NO: Nitric oxide; AD: Alzheimer's disease; PD: Parkinson's disease; HD: Huntington's disease; LPS: Lipopolysaccharide.

Correspondence:

Prof. Zhi-Shan Ding,
School of Medical Technology and Information Engineering, Zhejiang Chinese Medical University, Hangzhou 310053, Zhejiang, China.
E-mail: dzszjtcm@163.com
DOI: 10.4103/pm.pm_32_22

Access this article online
Website: www.phcog.com
Quick Response Code:

INTRODUCTION

As one of the most necessary immune effector cells in the central fearful device (CNS), microglia performs a key function in neuroinflammatory responses such as contamination and injury.[1] Excessive activation of microglia can lead to the overexpression of many inflammatory cytokines, such as interleukin-6 (IL-6), interleukin-1β (IL-1β), and tumor necrosis factor-alpha (TNF-α), which can damage nerve cells and cause neuroinflammation and various related diseases.[2,3] Hence, it is of terrific magnitude to restrain the immoderate manufacturing of pro-inflammatory cytokines in microglia for the duration of the therapy of CNS illnesses mediated using inflammation.

Lipopolysaccharide (LPS), as one of the components in Gram-negative bacteria's cell wall, can stimulate some cells to release a large number

Cite this article as: Sun T, Lu JJ, Wang BX, Ye XQ, Lan Li, Zhou FM, *et al.* Amygdalin attenuates neuroinflammatory injury via down-regulating toll-like receptors-2/toll-like receptors-4-nuclear factor kappa-B signaling pathway in BV2. Phcog Mag 2022;18:1096-103.

of inflammatory cytokines and nitric oxide (NO).[3,4] Toll-like receptors (TLRs) are necessary protein molecules in the immune response. TLR1–TLR10 have been found in the human body.[5] As the classic signal transduction pathways of the inflammatory response, TLR2 and TLR4 play an important role in inflammation.[6] Studies have shown that targeted inhibition of TLR2 and TLR4 can effectively reduce the degree of inflammation in the nervous system of mice.[7,8] LPS can bind to TLRs on the membrane of microglia to stimulate the activation of TLRs signaling pathways. After the TLRs signaling pathways are activated, they may bind to the downstream connexin myeloid differentiation primary response gene 88 (MyD88) and trigger the transcription of inflammatory signals. Then, nuclear factor kappa-B (NF-κB) is phosphorylated to make NF-κB enter the nucleus eventually.[9] NF-κB is an important nuclear transcription factor in the nucleus with a key role in the inflammatory response.[10] The activation of NF-κB can lead to the up-regulation of inflammatory cytokines such as IL-6, TNF-α, IL-1β, and so on.[11]

Oxidative stress and inflammation influence each other. Reactive oxygen species (ROS) is the main molecule produced in the process of oxidative stress. ROS can restrain the stimulation of NF-κB by inhibiting its upstream signal. Similarly, NF-κB can also affect the level of ROS by affecting the expression of antioxidant proteins.[12] Cyclooxygenase 2 (COX-2) is an inducible cyclooxygenase, which is hardly expressed in normal tissues, but highly expressed in inflammatory tissues. Kovarik *et al.*[13] found that the activation of TLR4 and TLR2 can induce the increase of COX-2 expression through their downstream signal pathways. Furthermore, inhibition of NF-κB signal activation can significantly reduce the expression of COX-2 in the mouse model of cerebral ischemia-reperfusion injury.[14]

Amygdalin is the main component of traditional Chinese medicine apricot kernel and peach kernel, which mainly has antitussive and anti-asthmatic effects, followed by anti-tumor, anti-fibrosis, anti-atherosclerosis, and other pharmacological effects.[15,16] Previous studies have shown that amygdalin also has anti-inflammatory effects.[17,18] For example, amygdalin can reduce the expression of inflammation-related cytokines such as IL-17A, IL-23, chemokine CCL2, and CCL5 in RAW264.7 cells induced by LPS.[18] Previous studies have found that amygdalin can inhibit the messenger ribonucleic acid (mRNA) overexpression of COX-2 and inducible nitric oxide synthase (iNOS) in LPS-stimulated BV2 mouse microglia (BV2).[17] However, there is no in-depth study on the effects of amygdalin on other aspects and inflammatory pathways.[19] On this basis, our study detected possible inflammatory signaling pathways and other related indicators. This study investigated the regulatory effect of amygdalin on LPS-induced inflammation in BV2 cells based on TLRs inflammatory pathways. At the same time, the results were further verified by the western blotting test at the protein level.

MATERIALS AND METHODS

Materials

Amygdalin powder was bought from Shanghai Yuanye Biotechnology Co., Ltd. (Shanghai, China, Lot: Z28A6L2815; purity: HPLC ≥98% storage conditions: 2-8°C).

Cell culture

In this study, BV2 cells were purchased from the typical Culture Preservation Center in China and maintained in Dulbecco's modified Eagle's medium (Gibco BRL, USA) containing 1% penicillin-streptomycin (Northrend, Hangzhou, China) and 10% fetal bovine serum (FBS; Cellmax) at 37°C in a 5% CO_2 humidified cell incubator.

Cytoactive detection

BV2 cells were cultured in a 96-well plate (5×10^4 cells/mL). At 70–80% confluence, BV2 cells were pre-incubated with amygdalin at the concentration of 1–100 μg/mL for 2 h and then uncovered to 1 μg/mL LPS (Sigma-Aldrich, St. Louis, MO, USA) for 24 h. After processing, BV2 cell morphology was observed and photographed underneath an optical microscope. Cell viability has measured the usage of 3-(4,5-dimethylthiazol-2-yl)-2,5-diphenyltetrazolin bromide (MTT [methyl thiazolyl tetrazolium]; Biofroxx, Germany). Briefly, the MTT solution was added to the 96-well plate with 10 μL per hole and incubated at 37°C for 4 h. After disposing of the medium, the formazan product was once dissolved in 200 μL dimethyl sulfoxide in every well. Absorbance values were measured at 560 nm with a microplate reader (Epoch 2 microplate enzyme labeling instrument, BioTek, USA).

Griess test

Nitrite in the cell culture media was measured as an index of NO production using the Griess assay package (Biyuntian, China). Cells were lysed and the supernatant was extracted. Then, 50 μL of supernatant was blended with the Griess reagents for 10 min at room temperature. The absorbance at 540 nm was measured by a microplate reader (Epoch 2 microplate enzyme labeling instrument, BioTek, USA).

Flow cytometry analysis

Cytokine levels were detected using the Cytometric Bead Array Mouse Th1/Th2/Th17 Cytokine Kit (BD Biosciences, San Diego, USA) according to the specification. The samples were analyzed using an Accuri™ C6 flow cytometer (Becton Dickinson, San Jose, CA, USA). The data were analyzed by BD FCAP Array™.

Total superoxide dismutase SOD activity detection

SOD activity is an index for evaluating the degree of oxidative stress injury of cells. Amygdalin (5–20 μg/mL) was added in advance for 2 h, and then LPS (1 μg/mL) was added to establish the model. After treatment for 24 h, the cells were lysed in accordance with the proportion of 200 μL SOD sample preparation solution added to 1×10^6 cells. The supernatant was obtained by centrifugation. WST-8/enzyme working solution and reaction initiation solution was prepared according to instructions. Samples, 2-(2-Methoxy-4-nitrophenyl)-3-(4-nitrophenyl)-5-(2,4-disulfophenyl)-2H-tetrazol ium Sodium Salt (WST-8)/enzyme working solution, and response initiation solution were delivered to the corresponding holes in sequence. After being incubated at 37°C for 30 min, the optical density (OD) value of 450 nm was detected by a multi-function enzyme labeling instrument (Epoch 2 microplate enzyme labeling instrument, BioTek, USA).

ROS activity detection

BV2 cells were pretreated with amygdalin (5–20 μg/mL) for 2 h and then LPS (1 μg/mL) was added to establish the model. After treatment for 24 h, the cells were washed with phosphate buffer saline (PBS). Then, 1 mL 10 μM 2',7'-Dichlorodihydrofluorescein diacetate (DCFH-DA) working solution was added to every well and incubated for 30 min in a cell incubator. The working solution was removed and the cells were washed with PBS 3 times to remove the residual probe. The plates were observed and photographed underneath an inverted fluorescence microscope (TI-s inverted fluorescence microscope, Nikon Co., Ltd., Japan.).

Quantitative real-time polymerase chain reaction (Q-PCR)

The cells have been positioned into tubes with TRIzol reagent™ (CWBIO, Beijing, China). RNA was separated by way of chloroform extraction

and isopropanol precipitation. Extracted RNA was dissolved in 20 μL RNase-free water and saved at −80°C. Complementary DNA (cDNA) was once synthesized using the BeyoRT™ II cDNA Synthesis kit (Biyuntian Biotechnology Co, Ltd, China). Copy number of rat genes was determined by Q-PCR using PowerUp™ SYBR™ Green Master Mix (Thermo Fisher Scientific, USA), following the specification. Data were amassed throughout every extension segment of PCR and analyzed using StepOnePlus™ Real-Time PCR instrument (Applied Biosystems, USA). RNA levels were normalized to glyceraldehyde-3-phosphate dehydrogenase (GAPDH) levels and calculated by the delta–delta threshold cycle (ΔΔCT). Primer sequences are shown in Table 1.

Western blotting

The cells were lysed with Radio Immunoprecipitation Assay (RIPA) buffer in the presence of cocktail protease inhibitors (pepstatin, leupeptin, aprotinin) and then centrifuged at 12,000 rpm for 15 min. The supernatant was gathered and the protein concentration was determined using a BCA assay. Then, loading buffer was added to the samples and heated at 95°C for 10 min.

Total protein from the supernatant was separated with the aid of 10% sodium dodecyl sulfate-polyacrylamide gel electrophoresis. The membranes were blocked by incubation with 5% bovine serum albumin in tris buffered saline-tween (TBS-T) buffer (10 mM Tris-HCl [TRIS hydrochloride], 150 mM NaCl, and 0.5% Tween-20) for 1 h at room temperature and then incubated with different primary antibodies overnight at 4°C. After washing, the membranes were incubated with horse radish peroxidase (HRP)-conjugated rabbit anti-goat secondary antibody for 2 h at 37°C, accompanied with the aid of washing. The bands were revealed using the ECL system (wanleibio, Beijing, China). The sign densities on the blots were measured with C-DiGit Blot Scanner (Molecular Imager, LI-COR company, USA) and normalized using anti-*β*-actin as an internal control (optical density detected protein/optical density internal control).

Table 1: Sequences of primers for a quantitative real-time reverse transcriptase-polymerase chain reaction

Gene	Sequence (5′-3′)	Product size (bp)
IL-6	Forward: CTC TGG TCT TCT GGA GTA CCA TAG	24
	Reverse: CCT TCT GTG ACT CCA GCT TAT C	22
IL-1β	Forward: CAT ATG AGC TGA AAG CTC TCC A	22
	Reverse: GAC ACA GAT TCC ATG GTG AAG TC	23
TNF-α	Forward: TCC CAA ATG GCC TCC CTC TC	20
	Reverse: TCG GCT GGC ACC ACT AGT TG	20
TLR4	Forward: AAG TGG CCC TAC CAA GTC TC	20
	Reverse: ATG GCA CCA TTG AAG CTG AG	20
TLR2	Forward: TCC GCG ACA TCC ATC ACC TG	20
	Reverse: AGA ACC GAG CCT CGG AAT GC	20
COX-2	Forward: CAG GCT GAA CTT CGA AAC A	19
	Reverse: GCT CAC GAG GCC ACT GAT ACC TA	23
GAPDH	Forward: GCA GTG GCA AAG TGG AGA TTG	21
	Reverse: GAC ACA GAT TCC ATG GTG AAG TC	23

IL-6=Interleukin-6; IL-1*β* = Interleukin-1*β*; TNF-*α* = Tumor necrosis factor-alpha; TLR4=Toll-like Receptor 4; TLR2=Toll-like Receptor 2; COX-2=Cyclooxygenase 2

Statistics

Statistical Package for Social Sciences version 22.0 software was used for statistical analysis, and the results were expressed by mean ± standard deviation (SD) ($\bar{x} \pm s$). One-way analysis of variance was used for comparison among groups. $P < 0.05$ was considered significant.

RESULTS

Establishment of inflammation model and screening of amygdalin concentration

After treatment, the content of nitrite in BV2 cells was detected after 6, 12, and 24 h, respectively. As shown in Figure 1A, after 6 h, all concentrations of LPS could not promote the increase of NO. After 12 h, 1 μg/mL LPS could significantly promote the production of NO ($P < 0.05$). After 24 h, compared with the normal control, all concentrations of LPS could significantly increase the level of NO ($P < 0.01$ or $P < 0.001$), and the effect of 1 μg/mL LPS stimulation for 24 h was the most obvious. Therefore, subsequent experiments were stimulated with 1 μg/mL LPS for 24 h to establish an inflammatory model in BV2 cells. After treatment with amygdalin, BV2 cell morphology was observed below an optical microscope [Figure 1B (a) - (e))] As shown in Figure 1B (f), amygdalin at concentrations of 1–100 μg/mL had no substantial impact on the viability of BV2 cells following LPS induction. As shown in Figure 1C, 1 μg/mL LPS induction for 24 h drastically accelerated the levels of NO in the supernatants of BV2 cells in contrast with the control group ($P < 0.01$). However, after treatment with amygdalin for 24 h, 5–20 μg/mL of amygdalin decreased the levels of NO while 40 μg/mL amygdalin treatment did decrease NO levels ($P < 0.05$ or $P < 0.01$). Therefore, amygdalin at concentrations of 5, 10, and 20 μg/mL was used for all subsequent experiments.

Amygdalin reduced the levels of IL-6 and TNF-*α*

As proven in Figure 2, 1 μg/mL LPS induction for 24 h notably improved the levels of IL-6 and TNF-*α* in the supernatants of BV2 cells in contrast with the control group (all $P < 0.05$). However, after therapy with amygdalin at the concentrations of 5, 10, and 20 μg/mL for 24 h, the levels of IL-6 and TNF-*α* were extensively decreased in the supernatants of LPS-induced BV2 cells ($P < 0.05$ or $P < 0.01$).

Amygdalin attenuated LPS-induced oxidative stress injury in BV2 cells

The impact of amygdalin on LPS-induced SOD expression in BV2 cells was shown in Figure 3. The level of SOD in the LPS group was extensively lower than that in the control group ($P < 0.05$). Compared with the LPS group, the levels of SOD in 5–20 μg/mL of amygdalin were substantially decreased ($P < 0.05$ or $P < 0.01$). To further study the effect of amygdalin on oxidative stress damage induced by LPS, the ROS levels were tested. The cells were treated with a DCFH-DA fluorescence probe and observed under a fluorescence inversion microscope. Results as shown in Figure 4 (a-f), in contrast with the control group, the green fluorescence intensity in the LPS group was drastically enhanced. The green fluorescence intensity in the treatment group decreased with the increase in concentration. At the same time, quantitative analysis of fluorescence showed that the fluorescence intensity of the model group was about 4 times that of the normal control group. However, after the administration of amygdalin, the fluorescence intensity could be significantly reduced to the normal level, or even lower. This showed that amygdalin

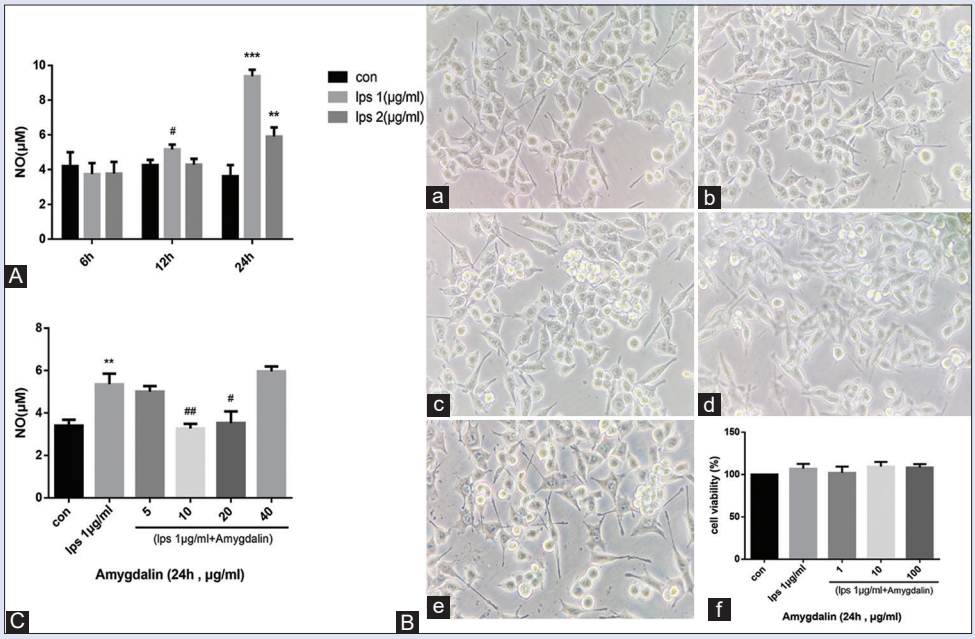

Figure 1: (A) The effect of different time and concentration of LPS on the content of NO in BV2 cells. Data are expressed as the mean ± SD ($n = 3$). # $P < 0.05$, versus control (12 h); ** $P < 0.01$, *** $P < 0.001$, versus Control (24 h). (B) Effect of amygdalin on cell morphology and cell viability of BV2 cells. Morphology of cells treated with normal medium (a), LPS 1 μg/mL (b), LPS 1 μg/mL + 1 μg/mL amygdalin (c), LPS 1 μg/mL + 10 μg/mL amygdalin (d), LPS 1 μg/mL + 100 μg/mL amygdalin (e) under an optical microscope (original magnification, 100×), viability of BV2 cells determined by MTT assay (f). Data are expressed as the mean ± SD ($n = 3$). (C) Effects of amygdalin on NO production of BV2 cells detected by Griess. Data are expressed as the mean ± SD ($n = 3$). ** $P < 0.01$, versus control; # $P < 0.05$, ## $P < 0.01$, versus LPS group

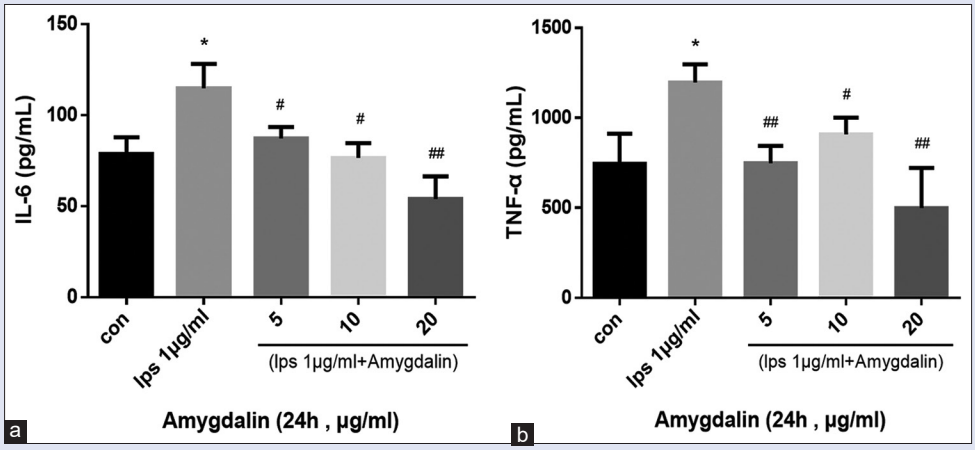

Figure 2: Effects of amygdalin pro-inflammatory factors in the culture supernatant of BV2 cells detected by flow cytometry. (a) IL-6 level; (b) TNF-*α* level. Data are expressed as the mean ± SD ($n = 3$). * $P < 0.05$, versus control; # $P < 0.05$, ## $P < 0.01$, versus LPS group

can limit ROS in BV2 cells in a concentration-dependent manner in a certain range. To sum up, it was suggested that amygdalin can reduce the oxidative stress damage induced by LPS to improve the antioxidant capacity of cells.

Amygdalin inhibited the expression of inflammation-related mRNA

Q-PCR is used to detect the key cytokines and pathway signals of amygdalin involved in inflammatory response at the level of mRNA. We examined the important substances that can increase after the occurrence of inflammation such as pro-inflammatory cytokines and the key cytotoxic factor COX-2 caused by inflammation. Their expression levels were notably improved in BV2 cells stimulated by LPS ($P < 0.01$ or $P < 0.001$; Figure 5). In contrast, throughout 24 h of amygdalin, the expressions of IL-1*β*, IL-6, TNF-*α*, and COX-2 mRNA were considerably reversed in BV2 cells stimulated by LPS ($P < 0.05$ or $P < 0.01$; Figure 5). At the same time, we also detected the main TLRs that trigger inflammation. The expression of TLR4 and TLR2 were significantly increased in BV2 cells stimulated by LPS ($P < 0.05$ or $P < 0.01$; Figure 5). Throughout 24 h of amygdalin, their levels of mRNA were notably reversed in BV2 cells stimulated by LPS ($P < 0.05$ or $P < 0.01$; Figure 5). These results showed that amygdalin relieved LPS-induced inflammatory response by inhibiting the up-regulation of IL-1*β*, IL-6, TNF-*α*, TLR4, TLR2, and COX-2 mRNA in BV2 cells.

Amygdalin downregulated the expression of proteins related to the TLR2/4 inflammatory pathway

MyD88 was a bridge linking TLR2 and TLR4 with their downstream signaling NF-κB. Phosphorylation of NF-κB may cause the accumulation of inflammatory-related substances such as pro-inflammatory cytokines, COX-2, and Recombinant NLR Family, Pyrin Domain Containing Protein3 (NLRP3). As proven in Figure 6, the western blotting experiment confirmed that LPS stimulation substantially improved the protein expression of TLR4, TLR2, MyD88, P-NF-κB p65, COX-2, and NLRP3 in BV2 cells (all $P < 0.05$). Nevertheless, most of the groups treated with amygdalin inhibited the protein expression of TLR4, TLR2, MyD88, P-NF-κB p65, COX-2, and NLRP3 in BV2 cells induced by LPS ($P < 0.05$ or $P < 0.01$).

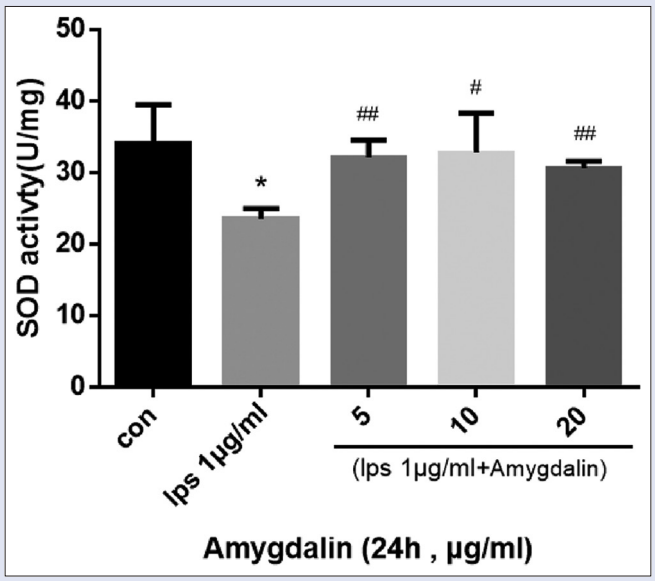

Figure 3: Effects of amygdalin on SOD production in BV2 cells detected by Total Superoxide Dismutase Assay Kit with WST-8 (WST-8 method). Data are expressed as the mean ± SD ($n = 3$). * $P < 0.05$ versus control; # $P < 0.05$, ## $P < 0.01$, versus LPS group

DISCUSSION

Neurodegenerative disease is a neurological disease with irreversible degeneration and loss of neurons in the brain and spinal cord. The etiology of most neurodegenerative diseases is unclear. The pathogenesis of this disease is complex, and the course of the disease is irreversible.[20] Neuroinflammation is the common pathogenic mechanism of many neurodegenerative diseases. Microglia play a key role in mediating central nervous system inflammation. The BV2 cells used in this study are a highly purified immortalized cell line obtained by transfection of mouse microglia. It retains the morphology, phenotype, and basic function of microglia and has been proved to be an ideal *in vitro* model for the study of microglia.[21]

The neurodegenerative disease has become an urgent problem to be solved all over the world. The characteristics of traditional Chinese medicine, such as small side effects, multi-targets, and multi-links, have great potential for the treatment of neurodegenerative disease. In this study, the results of the light microscope showed that amygdalin could reverse the morphological changes (round or amoeba phenotype) of BV2 cells induced by LPS to some extent. This showed that amygdalin can inhibit the activation of microglia.[22]

At present, LPS is recognized as the best iNOS inducer, which can cause cells to accumulate a large amount of NO, resulting in an inflammatory response.[23] The development of inflammatory diseases can be effectively controlled by regulating the content of NO. In this study, we screened out the best modeling time and dosage through different doses and

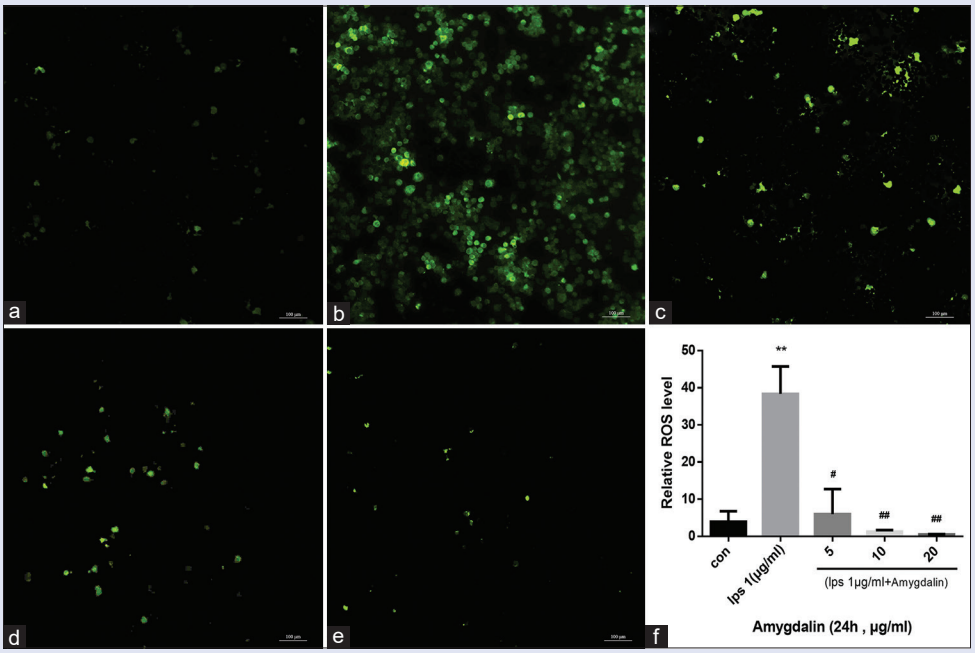

Figure 4: The activity of ROS in BV2 cells observed by inverted fluorescence microscope (original magnification, 40×). ROS of cells treated with normal medium (a), ROS of cells treated with LPS 1 μg/mL (b), ROS of cells treated with LPS 1 μg/mL + 5 μg/mL amygdalin (c), ROS of cells treated with LPS 1 μg/mL + 10 μg/mL amygdalin (d), ROS of cells treated with LPS 1 μg/mL + 20 μg/mL amygdalin (e). Data are expressed as the mean ± SD ($n = 3$). ** $P < 0.01$ versus control; # $P < 0.05$, ## $P < 0.01$, versus LPS group. Fluorescence quantitative results of ROS (f)

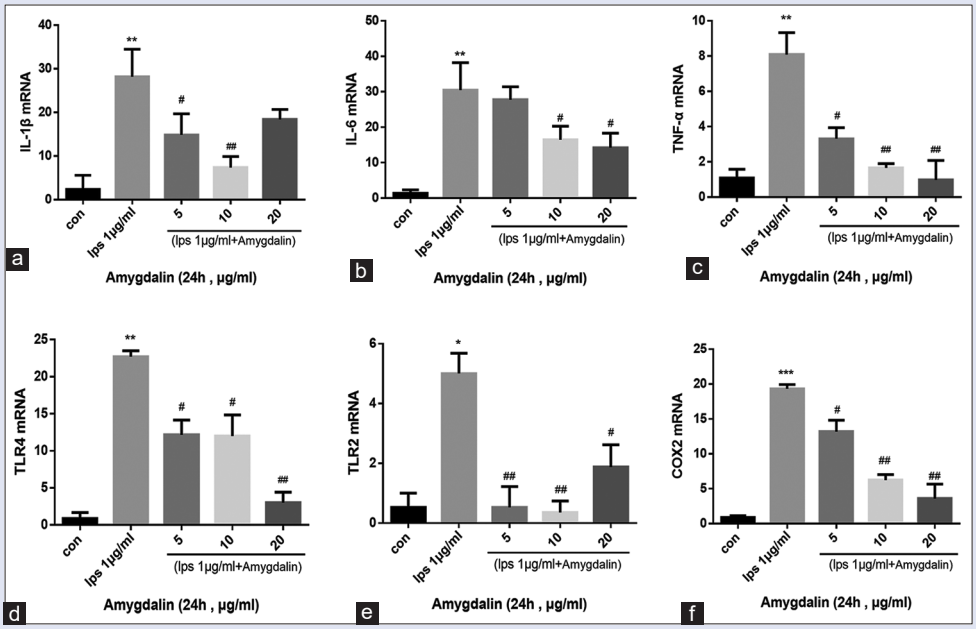

Figure 5: mRNA expression levels of IL-1*β*, IL-6, TNF-*α*, TLR4, TLR2, and COX-2 in BV2 cells stimulated by LPS after amygdalin treatment **(a-f).** Data are expressed as the mean ± SD ($n = 3$). * $P < 0.05$, ** $P < 0.01$, *** $P < 0.001$, versus control; # $P < 0.05$, ## $P < 0.01$, versus LPS group

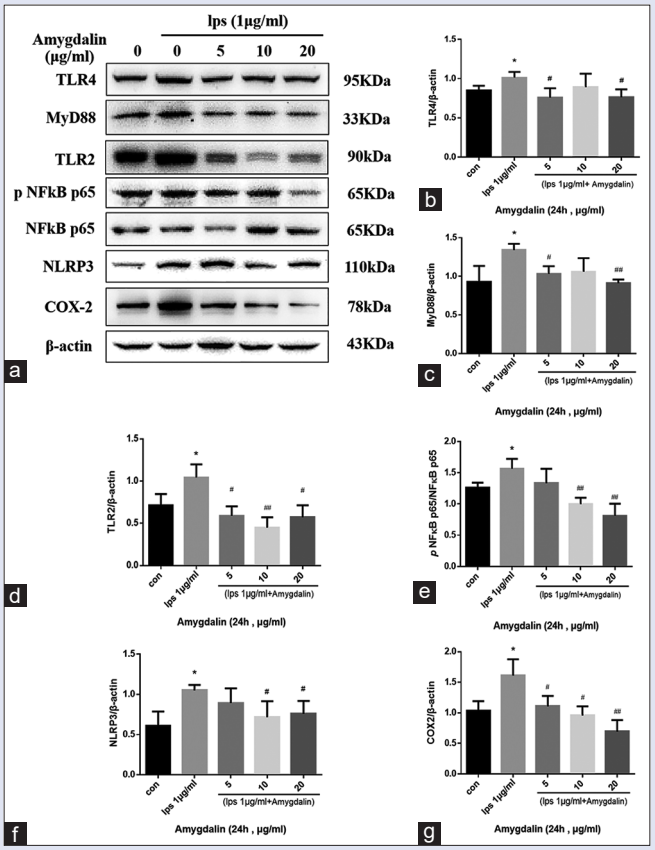

Figure 6: Amygdalin on the expression levels of TLR4, TLR2, MyD88, P-NF-κB p65, COX-2, and NLRP3 in LPS-treated BV2 cells detected by western blotting (a-g). TLR4, TLR2, MyD88, P-NF-κB p65, COX-2, and NLRP3 protein expression levels. Data are expressed as the mean ± SD ($n = 3$). *$P < 0.05$, versus control; # $P < 0.05$, ##$P < 0.01$, versus LPS group

various stimulation times. The results showed that when BV2 cells were stimulated by 1 μg/mL LPS, the content of NO reached the highest, which determined the modeling conditions. After that, this study found that 5–20 μg/mL amygdalin pretreated BV2 cells could significantly reverse the excessive production of intracellular NO induced by LPS. Therefore, we used this range of amygdalin concentration as the follow-up experimental concentration. Furthermore, the consequences of flow cytometry in this study showed that after pretreatment of BV2 cells with a certain concentration of amygdalin, the excessive release of IL-6 and TNF-*α* was significantly inhibited by LPS stimulation. At the same time, we also used the Q-PCR method to detect the expression of three important pro-inflammatory cytokines, IL-6, TNF-*α*, and IL-1*β*, at the gene level. The results also showed that amygdalin could inhibit the release of pro-inflammatory cytokines from BV2 cells induced by LPS to play a role in preventing inflammatory injury. These results were similar to the trend of anti-neuroinflammation *in vitro* by drugs such as Wasabi Extract, Limonin, and so on.[24,25]

SOD is one of the important substances in the oxidative stress reaction, which can remove excess superoxide anion, to protect cells from oxidative damage and inhibit inflammation. This study showed that BV2 cells pretreated with amygdalin can prevent the decrease of SOD level induced by LPS stimulation. Chen *et al.*[26] have shown the same trend, that is, increasing the content of SOD was beneficial to the recovery of nervous system injury.

Considering that ROS is the product of mitochondrial redox reaction, which performs a vital position in cellular signal transduction and *in vivo* balance. We detected ROS and proved that a certain concentration of amygdalin pretreated BV2 cells could reverse the excessive increase of ROS content induced by LPS. According to our results, some studies have shown that the production of ROS can be effectively reduced by down-regulating NF-κB.[27,28] Therefore, we speculate that its inhibitory effect on ROS may be related to the regulation of NF-κB pathway.

COX-2 is an important index in oxidative stress response. A previous study has shown that COX-2 was expressed in the whole process of

inflammation.[29] In this study, it was proved by western blotting and Q-PCR that amygdalin can reduce the excessive release of COX-2 in BV2 cells induced by LPS at the protein and gene level. In addition, previous studies have shown that many drugs can regulate the production of COX-2 through TLRs pathways to reduce the level of oxidative damage. For example, Bomfim *et al.*[30] discovered that the expression of COX-2 was considerably decreased after the use of anti-TLR4 antibodies in hypertensive animal models. Yoon *et al.*[31] have found that Chrysoeriol inhibited inflammation by decreasing LPS-induced COX-2 overexpression via the TLR4/MyD88 signaling pathway in Raw264.7 cells. These studies proved that there was a close relationship between TLRs and COX-2, which were in accordance with the results in the present study. Therefore, we speculate that amygdalin may inhibit LPS-induced COX-2 release by blocking the binding of TLR2/4 to its downstream signal COX-2 receptor.

TLRs, as one of the key factors in initiating natural immunity, can be recognized and activated by LPS.[32] Our results showed that amygdalin pretreatment can reduce the significant increase of TLR2 and TLR4 levels in BV2 cells induced by LPS, thus inhibiting their binding to the downstream connexin MyD88. And then it inhibited the inflammatory reaction caused by the activation of NF-κB, which is one of the important targets of anti-inflammatory effects. After activation, NF-κB can be phosphorylated and enter the nucleus. Then, it caused the increase of inflammatory cytokines and inflammatory corpuscle NLRP3 to aggravate the inflammatory response.[33] Some traditional Chinese medicine extracts such as icariin, puerarin, and hesperetin can inhibit LPS-induced cell inflammatory response by reducing NF-κB activation.[34-36] The results showed that amygdalin has the same trend in neuronal inflammation induced by LPS. Therefore, we inferred that the anti-inflammatory effect of amygdalin may be achieved by inhibiting the contact between TLR2/4 and MyD88. As a result, the phosphorylation level of NF-κB was further reduced. Finally, amygdalin reduced the excessive accumulation of pro-inflammatory cytokines, inflammatory corpuscles NLRP3, and oxidative damage, and then prevented the inflammatory response of BV2 cells induced by LPS stimulation.

CONCLUSION

In a word, this study explored for the first time the effects of amygdalin on inflammation-related cytokines, inflammatory pathways, and possible indicators related to oxidative stress in BV2 cells induced by LPS. As shown in the graphical abstract image, amygdalin may prevent LPS-induced neuroinflammatory injury and oxidative stress in BV2 cells through the TLR2/4-NF-κB signal pathway. However, the specific mechanism of amygdalin against neuroinflammation remains to be further studied.

Acknowledgements

The authors would like to thank all the teachers and fellow students of Ding Zhishan's research group for their guidance and help in the experiment and writing. The authors would also like to thank for the sponsorship of 2019YFC1708604, National Key R&D Program of China.

Financial support and sponsorship

This work was supported by a grant from the Biological basic study of supplementing Qi and activating Blood Circulation based on Vascular lesions and their components in the treatment of Cerebral Infarction/Cardiac Infarction (2019YFC1708604, National Key R&D Program of China).

Conflicts of interest

There are no conflicts of interest.

REFERENCES

1. Deczkowska A, Amit I, Schwartz M. Microglial immune checkpoint mechanisms. Nat Neurosci 2018;21:779-86.
2. Hickman S, Izzy S, Sen P, Morsett L, El Khoury J. Microglia in neurodegeneration. Nat Neurosci 2018;21:1359-69.
3. Rui Q, Cao S, Wang X, Duan X, Iao X, Dong W, *et al.* LMTK2 regulates inflammation in lipopolysaccharide-stimulated BV2 cells. Exp Ther Med 2021;21:219.
4. Yang H, Cheng X, Yang YL, Wang YH, Du GH. Ramulus Cinnamomi extract attenuates neuroinflammatory responses via downregulating TLR4/MyD88 signaling pathway in BV2 cells. Neural Regen Res 2017;12:1860-4.
5. Zhou XY, Liu J, Xu ZP, Fu Q, Wang PQ, Zhang H. Dexmedetomidine inhibits the lipopolysaccharide-stimulated inflammatory response in microglia through the pathway involving TLR4 and NF-κB. Kaohsiung J Med Sci 2019;35:750-6.
6. Hutchinson MR, Zhang Y, Brown K, Coats BD, Shridhar M, Sholar PW, *et al.* Non-stereoselective reversal of neuropathic pain by naloxone and naltrexone: Involvement of toll-like receptor 4 (TLR4). Eur J Neurosci 2008;28:20-9.
7. Kim D, Kim MA, Cho IH, Kim MS, Lee S, Jo EK, *et al.* A critical role of toll-like receptor 2 in nerve injury-induced spinal cord glial cell activation and pain hypersensitivity. J Biol Chem 2007;282:14975-83.
8. Piao Y, Gwon DH, Kang DW, Hwang TW, Shin N, Kwon HH, *et al.* TLR4-mediated autophagic impairment contributes to neuropathic pain in chronic constriction injury mice. Mol Brain 2018;11:11.
9. Liu T, Gao YJ, Ji RR. Emerging role of toll-like receptors in the control of pain and itch. Neurosci Bull 2012;28:131-44.
10. Ding RB, Chen P, Rajendran BK, Lyu X, Wang H, Bao J, *et al.* Molecular landscape and subtype-specific therapeutic response of nasopharyngeal carcinoma revealed by integrative pharmacogenomics. Nat Commun 2021;12:3046.
11. Chiu HF, Wang HM, Shen YC, Venkatakrishnan K, Wang CK. Anti-inflammatory properties of fermented pine (Pinus morrisonicola Hay.) needle on lipopolysaccharide-induced inflammation in RAW 264.7 macrophage cells. J Food Biochem 2019;43:e12994. doi: 10.1111/jfbc. 12994.
12. Zhang J, Wang X, Vikash V, Ye Q, Wu D, Liu Y, *et al.* ROS and ROS-mediated cellular signaling. Oxid Med Cell Longev 2016;2016:4350965.
13. Kovarik JJ, Hölzl MA, Hofer J, Waidhofer-Söllner P, Sobanov Y, Koeffel R, *et al.* Eicosanoid modulation by the short-chain fatty acid n-butyrate in human monocytes. Immunology 2013;139:395-405.
14. Bai S, Hu Z, Yang Y, Yin Y, Li W, Wu L, *et al.* Anti-inflammatory and neuroprotective effects of triptolide via the NF-κB signaling pathway in a rat MCAO model. Anat Rec (Hoboken) 2016;299:256-66.
15. Chen J, Hu Y, Mou X, Wang H, Xie Z. Amygdalin alleviates renal injury by suppressing inflammation, oxidative stress and fibrosis in streptozotocin-induced diabetic rats. Life Sci 2021;265:118835.
16. Jaszczak-Wilke E, Polkowska Ż, Koprowski M, Owsianik K, Mitchell AE, Bałczewski P. Amygdalin: Toxicity, anticancer activity and analytical procedures for its determination in plant seeds. Molecules 2021;26:2253.
17. Yang HY, Chang HK, Lee JW, Kim YS, Kim H, Lee MH, *et al.* Amygdalin suppresses lipopolysaccharide-induced expressions of cyclooxygenase-2 and inducible nitric oxide synthase in mouse BV2 microglial cells. Neurol Res 2007;29(Suppl 1):S59-64.
18. Xu X, Huang X, Zhang L, Huang X, Qin Z, Hua F. Adiponectin protects obesity-related glomerulopathy by inhibiting ROS/NF-κB/NLRP3 inflammation pathway. BMC Nephrol 2021;22:218.
19. Tanaka M, Toldi J, Vécsei L. Exploring the etiological links behind neurodegenerative diseases: Inflammatory cytokines and bioactive kynurenines. Int J Mol Sci 2020;21:2431.
20. Hou Y, Dan X, Babbar M, Wei Y, Hasselbalch SG, Croteau DL, *et al.* Ageing as a risk factor for neurodegenerative disease. Nat Rev Neurol 2019;15:565-81.
21. Dai XJ, Li N, Yu L, Chen ZY, Hua R, Qin X, *et al.* Activation of BV2 microglia by lipopolysaccharide triggers an inflammatory reaction in PC12 cell apoptosis through a toll-like receptor 4-dependent pathway. Cell Stress Chaperones 2015;20:321-31.
22. Lv B, Huo F, Zhu Z, Xu Z, Dang X, Chen T, *et al.* Crocin upregulates CX3CR1 expression by suppressing NF-κB/YY1 signaling and inhibiting lipopolysaccharide-induced microglial activation. Neurochem Res 2016;41:1949-57.
23. Wang Y, Xiang L, Wang Z, Li J, Xu J, He X. New anti-neuroinflammatory steroids against LPS induced NO production in BV2 microglia cells by microbial transformation of isorhodeasapogenin. Bioorg Chem 2020;101:103870.

24. Chen C, Yuanyuan Q. Effect of Wasabi extract on inflammatory response of BV2 cells induced by lipopolysaccharide. E3S Web of Conferences 2019,78:01011.
25. Lu S, Zhang J, Chen X, Mickymaray S, Liu Z. Limonin: A triterpenoid exerts protective effect during lipopolysaccharide stimulated inflammation in BV2 microglial cells. Pharmacogn Mag 2020;16:859-64.
26. Chen J, Chen W, Han K, Qi E, Chen R, Yu M, *et al.* Effect of oxidative stress in rostral ventrolateral medulla on sympathetic hyperactivity after traumatic brain injury. Eur J Neurosci 2019;50:1972-80.
27. Huang JH, Lan CC, Hsu YT, Tsai CL, Tzeng IS, Wang P, *et al.* Oridonin attenuates lipopolysaccharide-induced ROS accumulation and inflammation in HK-2 cells. Evid Based Complement Alternat Med 2020;2020:9724520.
28. Yoon JH, Kim O, Nam SW, Lee JY, Park WS. NKX6.3 regulates reactive oxygen species production by suppressing NF-kB and DNMT1 activities in gastric epithelial cells. Sci Rep 2017;7:2807.
29. Teismann P. COX-2 in the neurodegenerative process of Parkinson's disease. Biofactors (Oxf Engl) 2012;38:395-7.
30. Bomfim GF, Dos Santos RA, Oliveira MA, Giachini FR, Akamine EH, Tostes RC, *et al.* Toll-like receptor 4 contributes to blood pressure regulation and vascular contraction in spontaneously hypertensive rats. Clin Sci (Lond) 2012;122:535-43.
31. Yoon HS, Park CM. Chrysoeriol ameliorates COX-2 expression through NF-κB, AP-1 and MAPK regulation via the TLR4/MyD88 signaling pathway in LPS-stimulated murine macrophages. Exp Ther Med 2021;22:718.
32. Kumar J, Haldar C, Verma R. Melatonin ameliorates LPS-induced testicular nitro-oxidative stress (iNOS/TNFα) and inflammation (NF-kB/COX-2) via modulation of SIRT-1. Reprod Sci 2021;28:3417-30.
33. Xu WJ, Wang XX, Jin JJ, Zou Q, Wu L, Lv TF, *et al.* Inhibition of GGPPS1 attenuated LPS-induced acute lung injury and was associated with NLRP3 inflammasome suppression. Am J Physiol Lung Cell Mol Physiol 2019;316:L567-77.
34. Xiong W, Ma H, Zhang Z, Jin M, Wang J, Xu Y, *et al.* The protective effect of icariin and phosphorylated icariin against LPS-induced intestinal epithelial cells injury. Biomed Pharmacother 2019;118:109246.
35. Muhammad T, Ikram M, Ullah R, Rehman SU, Kim MO. Hesperetin, a citrus flavonoid, attenuates LPS-induced neuroinflammation, apoptosis and memory impairments by modulating TLR4/NF-κB signaling. Nutrients 2019;11:648.
36. Deng HF, Wang S, Li L, Zhou Q, Guo WB, Wang XL, *et al.* Puerarin prevents vascular endothelial injury through suppression of NF-κB activation in LPS-challenged human umbilical vein endothelial cells. Biomed Pharmacother 2018;104:261-7.